MOISTURE-INDUCED GOLD BALL BOND DEGRADATION OF POLYIMIDE-PASSIVATED DEVICES IN PLASTIC PACKAGES

C. Glenn Shirley
Intel Corporation
5200 N.E. Elam Young Pkwy.
MS: AL3-15
Hillsboro, OR 97124

Melissa Shell De Guzman
Intel Corporation
2200 Mission College Blvd.
P.O. Box 58119, MS: SC2-24
Santa Clara, CA 95052-8119

Abstract

A new mechanism of gold ball bond degradation in plastic packages has been demonstrated. Polyimide die topcoat and moisture stress accelerate bond degradation. The mechanism is further accelerated by mis-targeted bonds and "low" bonding parameters.

1. Introduction

Growth of intermetallic phases between gold and aluminum and incidence of Kirkendall voiding are major factors influencing the strength and reliability of gold ball bonds to aluminum bond pads. Intermetallic growth and bond degradation have been widely studied with accelerated life tests in both hermetic[1] and plastic[2] packages. The progression of growth of intermetallic phases depends on the environmental conditions (i.e., temperature and humidity), on the initial as-bonded morphology as determined by bonding parameters (i.e., ultrasonic power, dynamic bond force, temperature, and time), on the type of bond pad metallization, and on impurities and contamination on the bond pad surface [1,3,4]. For a given degree of intermetallic formation, the strength of a bond also depends on geometrical factors such as ball bond interfacial area and bond placement[5]. For example, a bond may be mis-targeted so that it overlaps the edge of a bond pad.

Polyimide passivation is known to improve die reliability in plastic packages by mechanical protection of the die surface. The incidence of thin film cracking, for example, is greatly reduced. However, new reliability jeopardies are possible, particularly relating to wire bonding:

- Polyimide etch residues or polyimide hydrolysis products generated in a humid ambient may influence intermetallic growth.
- Mis-targeted bonds overlapping polyimide may also interact with polyimide by either affecting the local bonding conditions, or by mechanical interactions during environmental stress.

To get a worst case look at these concerns, we ran small wire pull and preliminary bond shear experiments.. For the wire pull experiment, 120 polyimide-passivated units were bonded, half with centered bonds, and half purposely bonded 25% off of the bond pad. They were then assembled in 84 lead PQFP packages and subjected to either 80 hours of unbiased 156°C, 85% relative humidity (156/85) HAST or an 80 hour dry bake at 156°C. After stressing, molding compound was removed from the die and wires were pulled. Cumulative distributions of the pull strengths for 0% and 25% off-pad bonds following these stresses are shown in Figure 1.

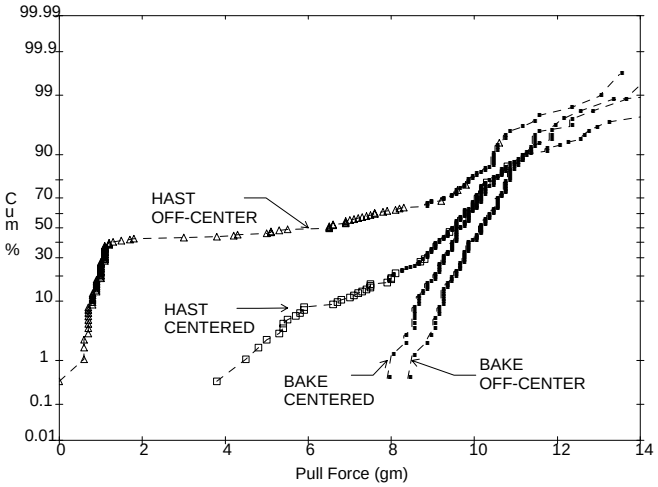

Fig. 1 Bond strength of polyimide topcoated plastic packaged units after 80 hours of 156/85 HAST or 156/0 bake. Open symbols: Ball lifts. Points: Wire breaks.

Two modes are indicated by plot symbols: A open symbol indicates a separation at the ball / bond pad interface, whereas a plotted point indicates a wire break. It can be seen that, without humidity, no intermetallic fractures occurred. The strength distribution characterizes wire breaks (mostly neck fracture) only, and is the same as is observed in unstressed units. In contrast, samples subjected to the same time-temperature conditions, but with 85% relative humidity moisture added, 20% to 60% of the bonds fail by intermetallic fracture at the ball/pad interface. Bonds mis-targeted by 25% have the higher proportion (60%) of such failures. Moreover, 40% of the bonds mis-targeted by 25% of the ball diameter were zero-strength. (The pull tester registers about 1 gram even for unattached wires.)

A preliminary shear test experiment was also performed by stressing units at 156°C for various times and at 0% (bake), 65%, and 85% relative humidity. A number of units and wires sufficient to establish the median shear strength were tested, with the results shown in Table I. It is clear that bonds are virtually undegraded after bakes for as long as 240 hours at 156°C, whereas addition of moisture to the stress leads to appreciably weaker bonds.

Table I Mean shear strength of interfacial fracture modes in grams after stress at 156°C for various times and relative humidities. Polyimide-passivated test dice.

	Hours at 156°C and x% Relative Humidity				
x % RH	40 hr	80 hr	120 hr	160 hr	240 hr
0%		102 g	104 g		91 g
65%		72 g		26 g	17 g
85%	52 g	26 g	19 g		

These observations prompted us to carry out a larger experiment to explore these issues in greater depth. Specifically, we considered the effects a polyimide topcoat, mis-targeting of bonds by various amounts, and ball bond process parameters. Since quantitative predictions of reliability require a mathematical model to describe these phenomena, destructive ball shear data were acquired for several accelerated environmental stress conditions, sufficient to extract probability distributions of shear strengths, and acceleration factor formulae which can be used to extrapolate the predictions of the model to conditions which actually occur in service.

There are at least four methods for studying bond degradation mechanisms: A simple electrical test for opens, Kelvin resistance measurements[6] , a bond wire pull test, and a ball shear test. Electrical continuity tests are not necessarily the best choice to determine ball bond integrity in plastic packages because even a separated bond can be held in contact with the bond pad by compressive stresses in the package. Kelvin measurements provide convenient information about kinetics of growth of intermetallic phases and voids at the Au/Al interface, but provide no direct information about the bond strength. Wire pull tests are convenient and quick, but only provide information about pathologically weak bonds, since wire strength is only about 10-12 grams. We therefore chose to use the bond shear test since it provides much more information about the bonds, in a mode similar to the way bonds are actually stressed in the plastic package.

In Section 2 we describe the fabrication and stress flow which produced the data. In Section 3 we describe the distribution of fracture modes as a function of the experimental variables to develop a qualitative understanding of the main effects of the variables. Section 4 presents an analysis of bond shear strength data leading to a quantitative reliability model for bond strength as a function of time, temperature, humidity, etc. Section 5 is an analysis of the effect of bonder parameters on Au/Al intermetallic integrity. The main conclusions are collected in Section 6.

2. Fabrication, Stress, and Test Flow

This study utilized SRAM die in 100 lead PQFP packages bonded on a K&S 1484XQ bonder. The passivation consisted of 0.6 micron of plasma silicon nitride. Additionally, some of the experimental units also had a four micron polyimide topcoat. Each die contained a number of repetitions of an off-pad bond matrix: Four consecutive bond pads were bonded with varying degrees of intentionally mis-targeted bonds; the bonds overlapped the pad edges by 0%, 5%, 15%, and 25% percent of the ball diameter. The polyimide was overetched to clear the pads, so only the 25% mistargeted bonds actually overlapped polyimide.

As noted by Hund[1], proper choice of bond parameters is vital to obtain reliable ball bonds. In the present study, ball bond time and temperature were fixed. The ball shear test was used to choose the best ultrasonic power and dynamic bond force windows meeting the strength and failure mode requirements as described in reference [7]. This methodology ensured that optimal ball bonds were made at the mid-point ("nominal") power/force bonder settings. Polyimide-passivated units with the off-pad bond matrix were bonded at the low power/low force ("low") corner of the bond window and at the high power/force ("high") corner as well as the mid-point settings. This was done to determine the sensitivity of mis-targeted bonds on polyimide to bond process window variations. Only the data from the midpoint bond settings were used to extract the reliability model. The effect of bond parameters will be discussed in Section 5.

The material fabrication and environmental testing flows are shown in Fig. 2. Some unmolded lead frames were taken from the production flow so that as-bonded bond strength data could be acquired. The packaged units were subjected to simulated board-mount stress ("preconditioning") consisting of 24 hours of bake at 125°C, followed by 5 cycles of temperature cycling condition "C", a 168 hour soak at 85/30, and 3 cycles of vapor-phase solder reflow. This was followed by a series of highly accelerated temperature/humidity/time stresses using a pressurized unsaturated temperature/humidity (HAST) chamber and a saturated steam test. Sample sizes varied at each readout; the short durations of the mild stresses had the largest sample sizes to increase the probability of observing failures.

The units intended for the 156/65 stress were inadvertently stressed at 156/85 for 17 hours before the mistake was noticed. This additional stress was taken into account in the extraction of a model.

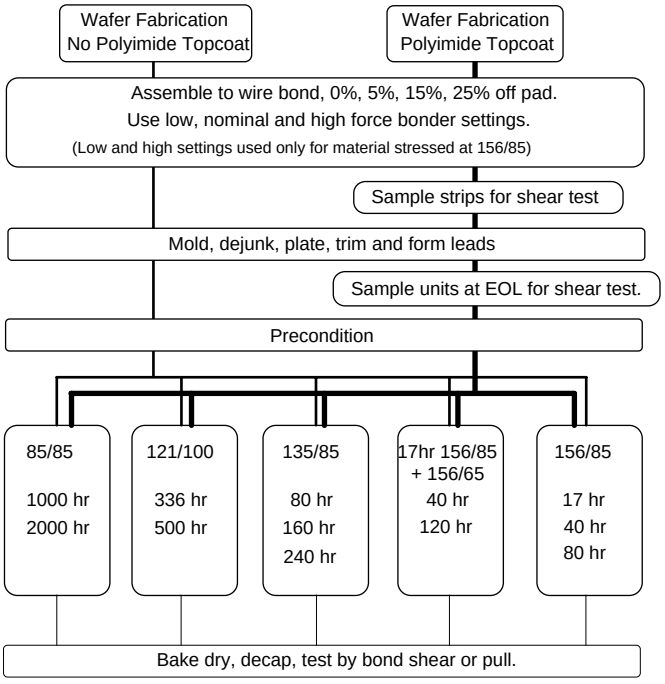

Fig. 2 Fabrication, environmental stress, and bond shear test flow for reliability model extraction.

Eight bonds per device were sheared, two of each degree of mis-targeting. The bonds failed either by ductile fracture of the ball, leaving gold on the bond pad ("gold" failure), or by fracture at the interface between the gold ball and the aluminum bond pad ("intermetallic" or "interfacial" failure). Virtually every bond sheared failed by one of these modes.

3. Fracture Mode Analysis

In this section we analyze the distribution of bond fracture modes obtained in the flow of Fig. 2 as a function of presence or absence of polyimide, degree of bond mis-targeting and the conditions and duration of environmental stress. In Fig. 3 we show the wire pull data acquired in the experiment. It is apparent that a combination of polyimide and mis-targeted bonding leads to significant bond degradation. We shall explore these effects more comprehensively, including the effect of environmental stress and time, by analysis of shear mode distributions.

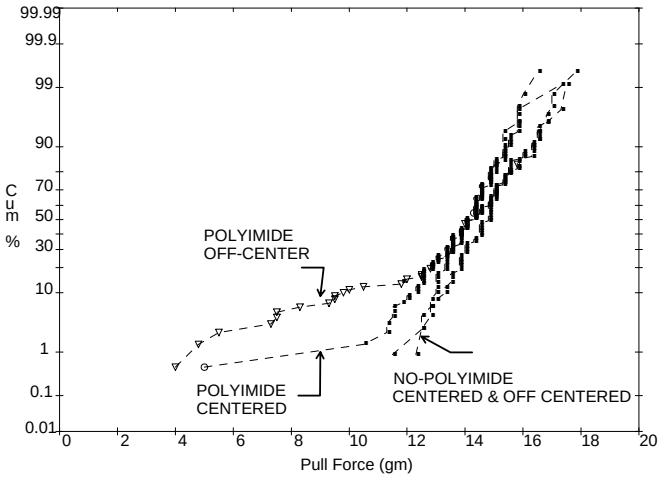

Fig. 3 Polyimide Vs non-polyimide 0% and 25% off-pad (bonded at nominal bonder settings) wire pull strengths after 40 hours of 156/85 HAST. Open symbols: Lifts due to interfacial fracture. Points: Wire breaks.

Although our primary focus is on the evolution of bond strength during environmental stress, it is interesting to study the variation in strength through the assembly process. This is shown in Table II.

Table II. Ball shear strength and modes for units with polyimide topcoat immediately after bond (Strip), at end of assembly (EOL), and after 40 hours of 156/85 HAST stress. Bonds with strength < 25 grams failing by either mode (in practise, only the Interface mode) are recorded as "Weak".

		Strength (gm)		Failure Mode Count		
Case	%Off Pad	Aver -age	Std Dev.	Ball Shear	Inter- face	Weak
Strip	0	68	5	1	99	0
Strip	25	66	7	1	99	0
EOL	0	109	7	93	7	0
EOL	25	95	12	66	34	0
HAST	0	67	9	18	82	0
HAST	25	43	15	0	81	19

When bonds are initially formed ("Strip" in Table II), 99% of failures are interfacial fractures with a mean strength of about 67 grams. At the end of assembly ("EOL" in Table II), the thermal processing through molding compound cure leads to an increased strength of the interface so that most bonds now shear by ductile deformation of the gold ball. As expected, mistargeted bonds show a lower incidence of ductile ball shear than centered bonds (66% versus 93%, respectively). Finally, after 40 hours of HAST stress, bonds again fail by interfacial fracture, but in contrast to the predominant mode just after assembly, 19% are "weak" (<25 grams.)[8]. This sequence of modes is caused by strengthening of the Au/Al interface by growth of intermetallic phase during the mild thermal history of cure, then subsequent degradation of the interface as Kirkendall voids form and coalesce during the more severe HAST stress.

When bonds were sheared, the maximum shear force and the failure mode were recorded. The way in which the two observed failure modes were distributed as a function of the experimental parameters is shown in Tables IIIA-E. The tables show the incidence of interfacial fracture for each degree of bond mistargeting, and for polyimide versus no-polyimide. The tables also show the incidence of "weak" bonds arbitrarily defined as bonds with shear strength less than 25 grams. For example, Table IIIB shows that for polyimide at 336 hours of steam (121/100), 11/36 25% off-pad bonds failed in shear test by interfacial fracture through the Au/Al intermetallic. The remaining 25/36 bonds failed in shear test by ductile shear through the gold ball. Moreover, none of the 336 hour steam, polyimide, 25% off-pad bonds (0/36) were weaker than 25 grams, irrespective of failure mode. In the tables, whenever a bond was weaker than 25 grams, it failed in test by the interfacial fracture mechanism.

Several conclusions can be made by inspection of Tables IIIA-F.

1. There is no statistical difference in failure mode incidence among 0%, 5%, and 15% off-pad cases for any environmental stress, with, or without polyimide. The 25% off-pad case, however, produced more interfacial fractures and weaker bonds than the rest of the population. Notable examples include 85/85 with polyimide in Table IIIA, and steam with polyimide in Table IIIB. Therefore, in the analysis of shear strengths in Section 4, the 0%, 5%, and 15% off-pad data are grouped together, and the 25% off pad data are treated as a separate group. The strength of the bonds decreased with increasing % off pad as shown in Table IIIF for a couple of examples, with the 25% off-pad bonds being significantly weaker than the others.

2. At early stress durations, there is a clear difference in the incidence of interfacial fracture between polyimide and no-polyimide. This is evident at the 1000 hour 85/85 readout where the polyimide case of 25% off-pad has 15/78 interfacial fractures, whereas the non-polyimide case of 25% off-pad has 0/48 interfacial fractures. This is also evident at all steam readouts, at the 240 hour 135/85 HAST readout, and the 40 hour 156/65 and 156/85 HAST readouts. The strength distributions for a couple of early readouts shown in Table IIIF clearly show that bonds in the polyimide case are weaker than in the non-polyimide case. SEM analysis (Fig. 4) showed that Kirkendall voids formed only on polyimide-passivated dice with all degrees of off-pad bonding following moisture stress at early readouts. The dice without polyimide topcoat, by contrast, did not show such voids. This result suggests that a polyimide etch residue or hydrolysis product activated during the moisture stress may be responsible for the void formation and consequent bond weakening. For longer stress times, a majority of bonds, with and without polyimide fail in test by interfacial fracture, and we will see in Section 4 that there is little difference between the strength distributions in polyimide and no-polyimide cases.

3. A high incidence of the interfacial fracture mode does not necessarily correspond to a high incidence of "weak" bonds. Nevertheless, as stress duration increases, interfacial fracture is a precursor to weak bonds. In fact, the initial formation of intermetallic phase actually strengthens the Au/Al interface. But with increasing stress duration and further growth of the intermetallic phase, Kirkendall voids form and coalesce, ultimately weakening the bond. This effect is seen in Table IIID.

Table IIIA 85/85, nominal bonder settings.

		Polyimide		No Polyimide	
	% Off Pad	1000 Hours	2000 Hours	1000 Hours	2000 Hours
Interfacial	0	2	0	0	0
	5	1	0	0	0
	15	2	0	0	0
	25	15	2	0	0
Bonds < 25 grams	0	0	0	0	0
	5	0	0	0	0
	15	0	0	0	0
	25	0	0	0	0
Sample Size		78	48	48	28

Table IIIB Steam (121/100), nominal bonder settings.

		Polyimide		No Polyimide	
	% Off Pad	336 Hours	500 Hours	336 Hours	500 Hours
Interfacial	0	0	3	0	0
	5	1	4	0	0
	15	1	9	0	0
	25	11	13	0	5
Bonds < 25 grams	0	0	0	0	0
	5	0	0	0	0
	15	0	0	0	0
	25	0	0	0	0
Sample Size		36	22	22	14

Tables IIICa 135/85 HAST, nominal bonder settings, polyimide.

		Polyimide			
	% Off Pad	80 Hours	160 Hours	240 Hours	320 Hours
Interfacial	0	0	6	10	19
	5	0	3	10	18
	15	2	3	17	22
	25	1	6	22	22
Bonds < 25 grams	0	0	0	0	0
	5	0	0	0	0
	15	0	0	0	0
	25	0	0	0	0
Sample Size		28	26	26	22

Tables IIICb 135/85 HAST, nominal bonder settings, no polyimide.

		No Polyimide			
	% Off Pad	80 Hours	160 Hours	240 Hours	320 Hours
Interfacial	0	0	1	2	9
	5	0	1	6	11
	15	0	1	7	13
	25	0	1	4	12
Bonds < 25 grams	0	0	0	0	0
	5	0	0	0	0
	15	0	0	0	0
	25	0	0	0	0
Sample Size		18	16	14	14

Table IIID 17 hours of 156/85 + 156/65 HAST, nominal bonder settings.

		Polyimide		No Polyimide	
	% Off Pad	40 hours	120 hours	40 hours	120 hours
Interfacial	0	27	36	0	22
	5	30	36	0	22
	15	36	36	0	22
	25	39	36	0	22
Bonds < 25 grams	0	0	9	0	5
	5	0	10	0	6
	15	0	14	0	7
	25	0	17	0	13
Sample Size		48	36	30	22

Table IIIE 156/85 HAST, nominal bonder settings.

		Polyimide			No Polyimide		
	% OP	17 hrs	40 hrs	80 hrs	17 hrs	40 hrs	80 hrs
Interfacial	0	1	26	30	0	0	11
	5	0	21	30	0	1	11
	15	0	29	30	0	3	11
	25	2	30	30	0	4	12
Bonds < 25 grams	0	0	0	0	0	0	0
	5	0	0	0	0	0	1
	15	0	0	1	0	0	0
	25	0	0	1	0	0	3
Sample Size		60	30	30	38	16	12

Table IIIF Ball shear strengths for selected HAST stresses, nominal bonder settings.

		Polyimide		No Polyimide	
	% OP	Mean	Std. Dev.	Mean	Std. Dev.
17 hrs 156/85 + 40 hr 156/65	0	63.5	6.6	75.5	4.2
	5	59.9	6.8	74.1	6.1
	15	58.6	7.9	71.2	7.8
	25	54.3	8.6	68.3	6.3
40 hr 156/85	0	63.8	7.2	70.2	4.0
	5	63.8	7.1	70.2	5.1
	15	60.2	4.8	65.8	9.6
	25	57.6	5.7	64.9	5.7

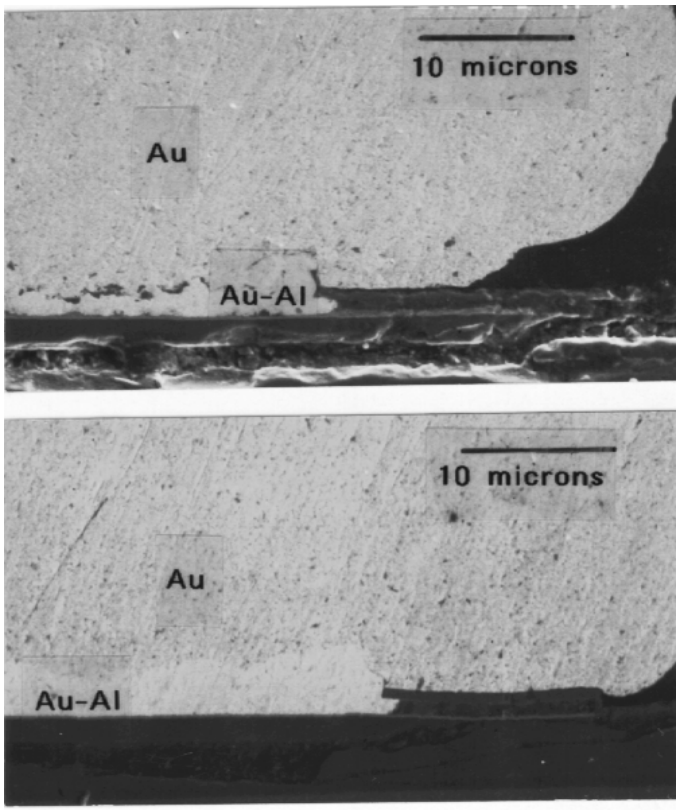

Fig. 4. Cross section of 25% off-pad ball bonds after 40 hours of 156/85 HAST. Top: With polyimide topcoat. Bottom: Without polyimide topcoat. Kirkendall voiding is associated only with the polyimide case.

4. Reliability Model Extraction

In this section we analyze quantitative shear strength data acquired in the flow shown in Fig. 2, with the objective of extracting a model that can be used to predict bond reliability. Although wire pull data show the effect of polyimide, mis-targeting and moisture in a qualitative way, the data is not as useful as shear data in extracting a quantitative reliability model. There are two reasons for this: (1) The interfacial fracture mode of interest is severely censored by the strength of the wire. That is, only very severely degraded Au/Al interfaces will fracture when tested by this method - so we are deprived of information about early stages of degradation. (2) In plastic packages, the main stress applied to bonds by the molding is a shearing stress[9]. Thus, a model based on shearing data is closely related to the actual stress on the bonds in a plastic package.

When each bond is shear tested, the strength and failure mode are recorded. If the interface between the gold ball and the aluminum pad is sufficiently strong, the ball will fail by ductile shear through the gold ball, leaving gold on the pad. The shear strength recorded for this ductile ball shear mode provides only a lower bound on the strength of the interface. On the other hand, if the Au/Al interface is weaker than the stress required to cause ductile shearing of the gold ball, then the interface will fracture by shear, and the strength recorded is an actual measure of the strength of the interface. We wish to know the distributions of the Au/Al interface strengths as if there were no censoring by the ductile gold ball shear mechanism obscuring observation of stronger interfaces. We employed Nelson's[10] method of hazard plotting analysis to separate the strength distributions of the two competing, mutually censoring failure modes.

We chose to plot the shear strength data on lognormal probability plots since this avoids the issue of extrapolation to negative bond strengths, which would be physically implausible.. We grouped the 0%, 5%, and 15% off-pad data since, as shown in the mode analysis in Section 3, there was no observable dependence on the degree of mis-targeting up to 15% off pad. The 25% off pad data were treated as a separate group. 52 lognormal distribution plots were made with the separated gold ball shear and interfacial fracture distributions superimposed. Straight lines were fitted by the least-squares method through each of the distributions to determine the value of the median shear strength and sigma. A range of values for sigma was found for each shear fracture mechanism. We found

$\sigma = 0.07 \pm 0.02$ (Au ball shear mechanism)

$\sigma = 0.17 \pm 0.07$ (Interfacial fracture mechanism).

We assumed one value (the median value) of sigma for each mechanism, and made slope-constrained least-squares fits to the distributions using the median values of sigma. Examples of distribution plots, and sigma-constrained distributions are given in Fig. 5 for the case of 25% off-pad, polyimide-passivated material stressed at 135/85. The values of the median shear strengths of interfacial fracture, F_{50}, were thus determined as a function of temperature, humidity, time in stress, degree of passivation overlap, and whether or not the die had a polyimide overcoat.

The next step was to determine a functional dependence for the time variation of the median interfacial shear strength. We noticed from a log-log plot of F_{50} versus time that F_{50} is approximately inversely proportional to time at relatively long stress times. However, F_{50} cannot be inversely proportional to time for all times, since for short times this would predict a strength increasing without limit, in violation of the fact that the interface between the gold ball and the aluminum pad will have a finite strength at zero time in stress. We explored several functions which had the appropriate asymptotic behavior for long and short times, choosing the simplest. The polyimide data are well described by the following function:

$$F_{50} = \frac{1}{\sqrt{(at)^2 + 1/b^2}} \quad \text{(Polyimide)} \qquad (1)$$

where a is the time acceleration factor, and b is the limiting initial bond strength. This is shown in Fig. 6, where polyimide data (solid symbols) are seen to fall on straight lines on a plot of $1/(F_{50})^2$ versus t^2 for a 135/85 HAST stress. This was also observed for other stresses. It is also clear from Fig. 6 (and other similar plots) that the time dependence of F_{50} for long stress times was similar for polyimide and non-polyimide, but different for 25% mistargeted bonds and < 25% mis-targeted bonds.

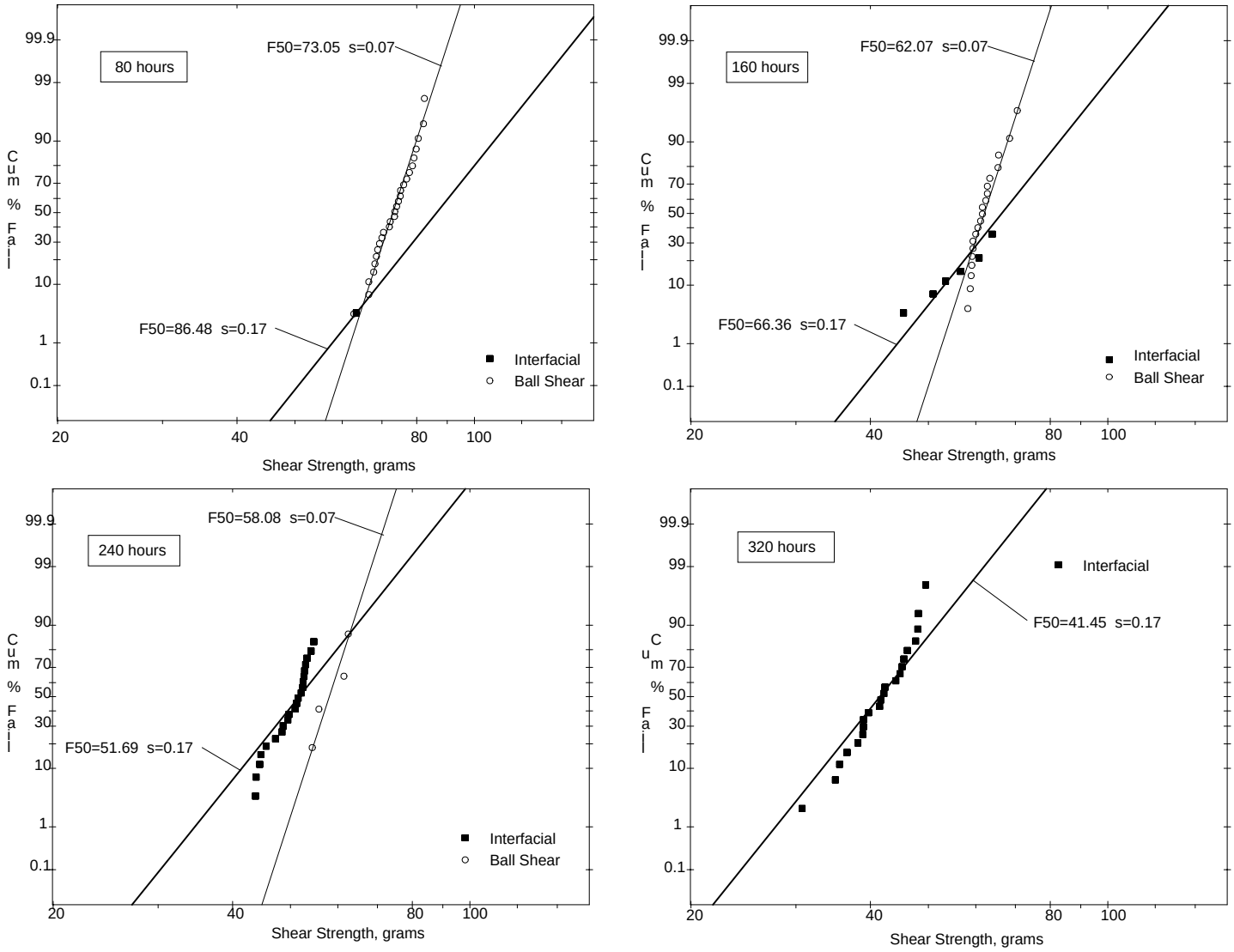

Fig. 5 Bond shear strength distributions for polyimide-passivated material with 25% overlap of the bond onto passivation, as a function of time at 135/85 HAST. With increasing stress duration the distribution of interfacial shear strengths shifts to smaller values, whereas the gold ball ductile fracture strength distribution remains relatively unchanged. Thus, the incidence of interfacial fractures increases with increasing stress duration. The fitted distributions are slope-constrained to represent, for each mode, a single value of sigma which is optimal for *all* of the strength distribution data (48 other plots besides those shown here).

It is reasonable to expect the same time-zero interfacial strength for polyimide and no polyimide. Thus the polyimide and non-polyimide cases appear to have the same asymptotic time dependence for short and long stress times. On the other hand, we can see from Tables III that at intermediate stress times the incidence of interfacial fracture is greater for polyimide than for non-polyimide. This corresponds to the missing non-polyimide data points (open symbols) at the earliest readout time in Fig. 6. One way to describe this effect is to choose a parameter $n>2$ in the formula

$$F_{50} = \frac{1}{\sqrt[n]{(at)^n + 1/b^n}} \quad \text{(Non-Polyimide, } n>2, \; n=3 \text{ chosen)} \quad (2)$$

The data were not sufficient to determine an unequivocal value for *n*, except to say that it was larger than 2. We have chosen a value $n=3$ which gives a reasonable qualitative description of the non-polyimide time dependence.

As a result of fitting all of the median shear strength data to functions of the form of Eqs. (1) and (2), we found that the zero-stress strength of bonds was well represented by b = 98.3 grams for the 25% mis-targeted bonds, and by b = 112.7 grams for all the bonds mis-targeted by less than 25%, irrespective of whether the passivation included polyimide or not. The values of the acceleration parameter, *a*, were also determined for each environmental stress condition, each polyimide versus no-polyimide case, and each case of bond mis-targeting.

We have seen in Table I that in a dry ambient (bake, relative humidity = 0) the Au/Al interface strength does not degrade appreciably even at the highest stress temperature (156°C) for the times of interest in this experiment (up to 120 hours in 156/65, and 80 hours in 156/85). Therefore, it is reasonable to assume an acceleration parameter which goes to zero as the relative humidity goes to zero. The "Peck" [11] formula has this property, and has been widely used to describe the acceleration of moisture-related failure

mechanisms. Of course, baking (0% relative humidity) will eventually degrade the Au/Al interface by Kirkendall voiding, but at much longer times than are observed in the present study. This "thermal activation only" mechanism is therefore not the subject of this paper.

For each case of polyimide versus no polyimide and degree of bond mis-targeting, the acceleration parameter a was fitted to the Peck formula

$$a = a_0 \times h^p \times \exp(-Q / kT) \quad (3)$$

where h ($0<h<1$) is the relative humidity and the constants a_0, p and q were determined by a least-squares fit to the data[12]. The constants found are given in Table IV.

Table IV. Acceleration model parameters in acceleration formula, Eq. (3).

Poly-imide?	% Off Pad	a_0 (gm-hrs)$^{-1}$	p	Q (eV)
Yes	< 25%	3.380E10	0.82	1.19
Yes	25%	8.638E9	1.05	1.13
No	< 25%	2.581E10	1.20	1.17
No	25%	2.795E10	0.85	1.09

It is apparent that one activation energy can describe all four cases of polyimide and no-polyimide. Also, a sensitivity study shows that the indicated variations in p of +/- 0.2 do not greatly affect the fit of the model. Therefore, we took averages of p and Q from Table III and re-determined a_0 for each case with the constraint that p = 0.98 and Q = 1.15 eV.

Therefore, the complete model describing the degradation of the median interfacial strength is embodied in Equations (1), (2), and (3) with the parameters shown in Table V.

Table V. Interfacial strength degradation model for Au/Al bonds, made at nominal bonder power/force settings in temperature/humidity ambients. Z_P is the Pth percentile of the normal probability function.

Poly?	% Off Pad	n	b (gm)	a_0 (gm-hrs)$^{-1}$	p	Q (eV)
Yes	< 25%	2	112.7	1.130E10	0.98	1.15
Yes	25%	2	98.3	1.338E10	0.98	1.15
No	< 25%	3	112.7	1.215E10	0.98	1.15
No	25%	3	98.3	1.492E10	0.98	1.15

$$F_{50} = \frac{1}{[(at)^n + 1/b^n]^{1/n}}$$

$$a = a_0 \times h^p \times \exp(-Q / kT)$$

$$F_P = F_{50} \times \exp(-\sigma \times Z_P)$$

$$\sigma = 0.17$$

In Fig. 7 we plot the experimental values of the acceleration constant a, scaled to take into account thermal effects, versus humidity. That is, we plot

$$A = a \times \exp(Q / kT) \quad (4)$$

versus h. From Eq. (3) with p = 0.98, this should be almost proportional to h, and we see in Fig. 7 that the data are consistent with this functional dependence.

We demonstrate the overall fit of the model to the data by superimposing the model predictions over the experimental values of the median shear strength of the Au/Al interface in Fig. 8

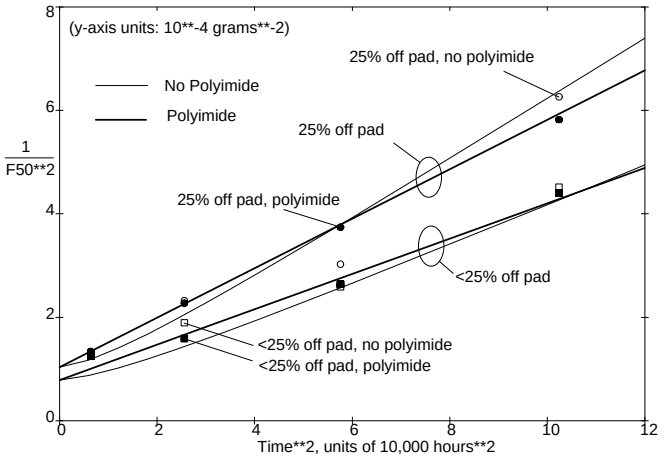

Fig. 6 Median shear strength of bond interface as a function of time in 135/85 HAST. A linear plot corresponds to the functional form of Eq. (1). The intercept is b and the slope is a^2. The circular filled plot symbols correspond to the data of Fig. 5.

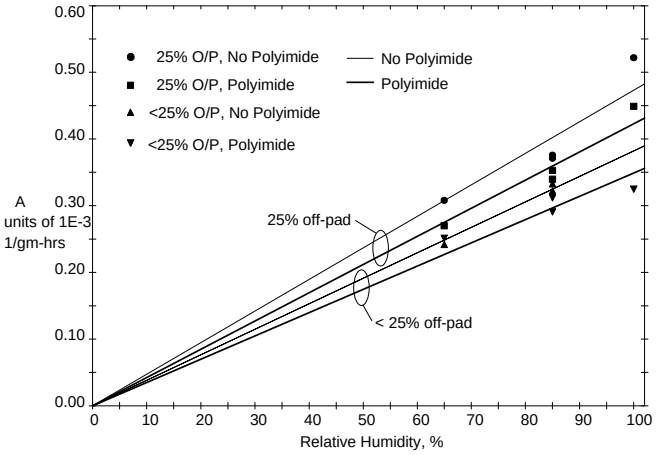

Fig. 7 Acceleration factors, a, temperature-normalized to 156°C, using activation energy of Q = 1.15 eV, to isolate the relative humidity dependence of acceleration. Shows that acceleration is proportional to relative humidity.

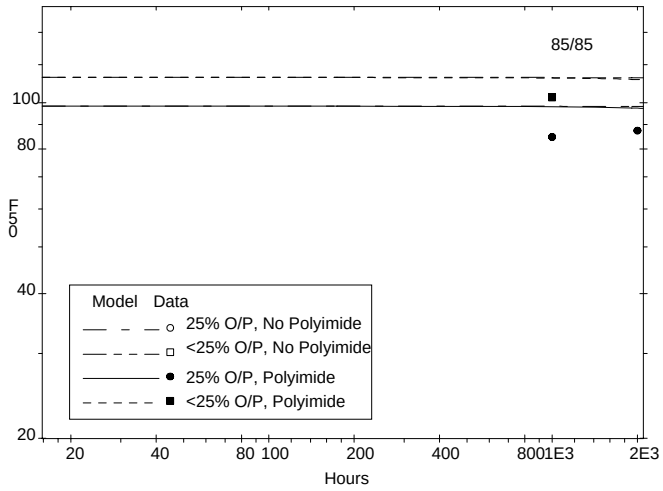

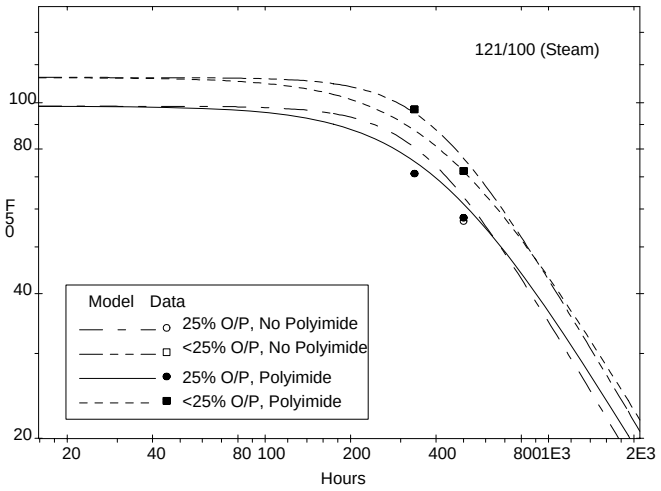

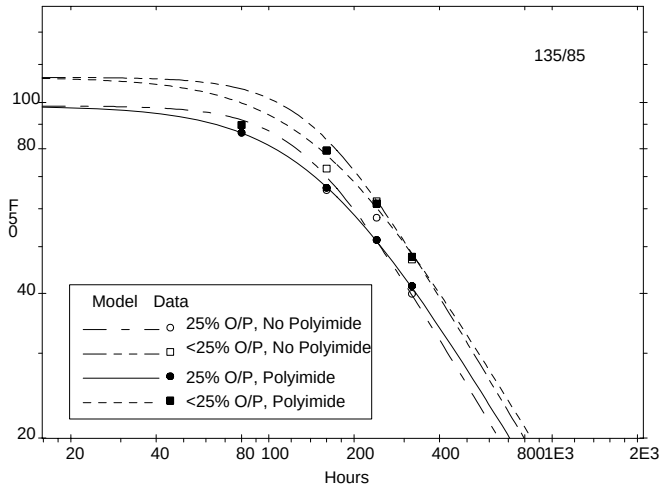

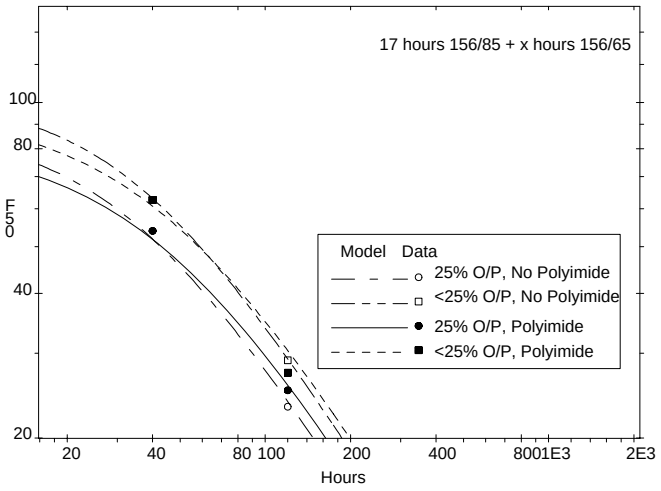

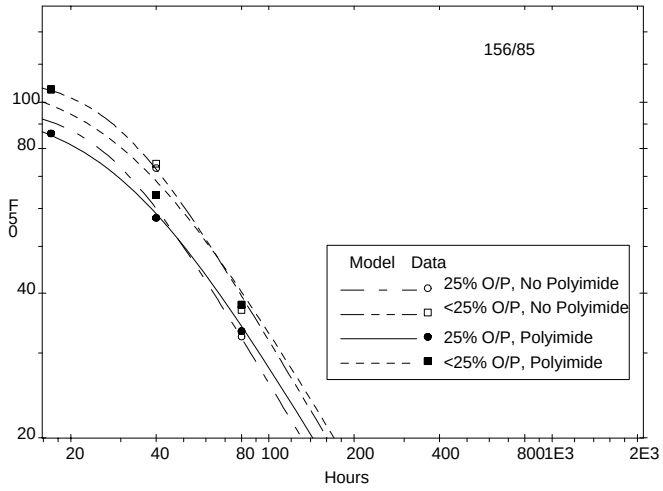

Fig. 8 Au/Al interfacial shear strength in grams as a function of stress ambient and time for various percentages of bond mis-targeting, and polyimide versus no polyimide. Predictions of the model in Table V are superimposed on the median interfacial shear strengths derived from distributions such as shown in Fig. 5.

5. Effect of Bonder Parameters on Au/Al Intermetallic Degradation

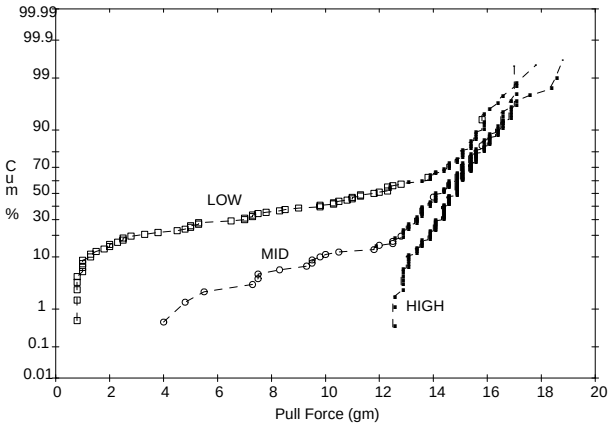

Fig. 9 Effect of bonding parameters on HAST-induced (40 hours of 156/85) weakening of worst-case bonds (25% off-pad, with polyimide). Wire pull results. Open symbols: Lifts. Points: Wire breaks.

Table VI 156/85, high and low bonder settings.

		Polyimide, low bonder parameters		Polyimide, high bonder parameters	
	% OP	40 hr	80 hr	40 hr	80 hr
Interfacial	0	30	12	11	40
	5	30	12	17	39
	15	30	12	16	39
	25	30	12	29	40
Bonds < 25 grams	0	1	3	0	0
	5	1	3	0	0
	15	2	7	0	0
	25	16	10	0	0
Sample Size		30	12	40	40

As mentioned in Section 2, wire pull and bond shear data were collected following 40 and 80 hours of 156/85 HAST on polyimide lots bonded at the low and high ends of the ultrasonic power/bond force window as well as at the midpoint settings. The wire pull force distributions for each of the bonder settings are shown in Fig. 9. The slight decrease in median pull strength (3 grams) and large increase in standard deviation for low bonder settings is seen to be associated with a greatly increased incidence of ball lifts. Table IIIE, which lists ball shear data for nominal bonder parameters can be compared with Table VI which shows comparable data for low and high bonder parameters. Comparison of these tables shows that polyimide interfacial fracture rates are extremely sensitive to bonding conditions; higher bond power/force settings produce fewer intermetallic failures and higher bond strengths.

Tables VI and IIIE show that after 40 hours of 156/85, the low bonder settings produced 100% intermetallic failures (inclusive of all degrees of mis-targeting), indicating inadequate mixing of the gold ball and aluminum pad. Increasing the ultrasonic power and bond force to their mid-point settings improved this failure rate slightly to 88.3%. The incidence of intermetallic fractures was further reduced to 46% when the high end of the power/force window was used. As seen in Table IIIE, however, the samples without polyimide had the least amount of ball/bond separations; 12.5% overall for 40 hours of HAST.

6. Discussion and Conclusions

Effect of Polyimide. In the first stages of bond degradation (up to about 30% degradation of bond strength) presence of polyimide is associated with increased frequency of interfacial fracture and generally weaker bonds. Polyimide etch residues or hydrolysis products may have been responsible for the higher incidence of Kirkendall voiding that leads to bond degradation. At the later stages of bond degradation, when bond strengths have degraded by 30% to 70 grams or more, bonds on polyimide and non-polyimide material degrade at the same rate.

Effect of Mistargeted Bonds. Bond mistargeting has a strong effect on the incidence of intermetallic fracture for both polyimide and non-polyimide passivated materials. This increased incidence of intermetallic fracture is related to the fact that bonds with greater mistargeting are weaker and are less likely to be censored by the ductile ball shear mode. Bond strength decreased with increasing bond mistargeting for any given stress history, both with and without polyimide.

Effect of Processing. Bond strengths immediately after bonding increase by about 50% during post mold cure due to formation and growth of the Au-Al intermetallic phases at the ball/bond pad interface. Further growth of the intermetallic phase during environmental stressing leads to weakening of the interface due to Kirkendall void formation and coalescence.

Effect of Bonder Power/Force Settings. The bond integrity of polyimide-coated samples was strongly influenced by the ultrasonic power and bond force. The higher end of the bond window produced the strongest ball bonds**.**

Time Dependence of Degradation. The strength of bonds on polyimide-passivated material degrades with time according to the relationship

$$F_{50} = \frac{1}{\sqrt{(at)^2 + 1/b^2}}.$$

For non-polyimide coated material, the as-formed bonds have the same strength as on the polyimide coated material. At long stress times, the bond strength of polyimide and non polyimide material also has the same asymptotic time dependence (inversely proportional to time). However, the time dependence of strength at early stress times is different between polyimide and non-polyimide material as evidenced by the higher frequency of intermetallic fracture for polyimide. Paucity of non-polyimide shear strength data at early times prevented an accurate determination of the functional dependence.

Acceleration Model. Thermal effect of bond degradation was described for both polyimide and non-polyimide cases by an activation energy of Q = 1.15 eV. The effect of moisture was described for all cases by a proportionality of the acceleration factor to relative humidity. All the degradations observed in this study depended on the presence of moisture, since if humidity were not present, even the highest temperature/time stress used in this study would show virtually no degradation of bond strength.

Reliability Predictions of Model. The reliability model summarized in Table V can be used in conjunction with the results

of package mechanics calculations of shear stress applied to the ball bonds in a plastic package. For example, if it were known that the shear stress applied to a bond would never exceed, say, 25 grams in service, and we have a reliability requirement of, say, 1 bond per million with interfacial fracture, then it is possible to use the model in Table V to calculate the time until this requirement is violated. Loci of constant times to failure are plotted as contours in the humidity-temperature plane in Fig. 10. The parameters for the 25% off-pad polyimide case were used.

It can be seen in Fig. 10 that the time to failing the reliability requirements we have set in the example is greater than 10^7 hours (more than 1000 years!) for typical service ambients. Thus, while the moisture-induced bond failure mechanism discussed in this paper is much more accelerated than the well-known purely thermal failure mechanism (accelerated by baking), nonetheless the moisture-induced mechanism does not pose any serious reliability jeopardy.

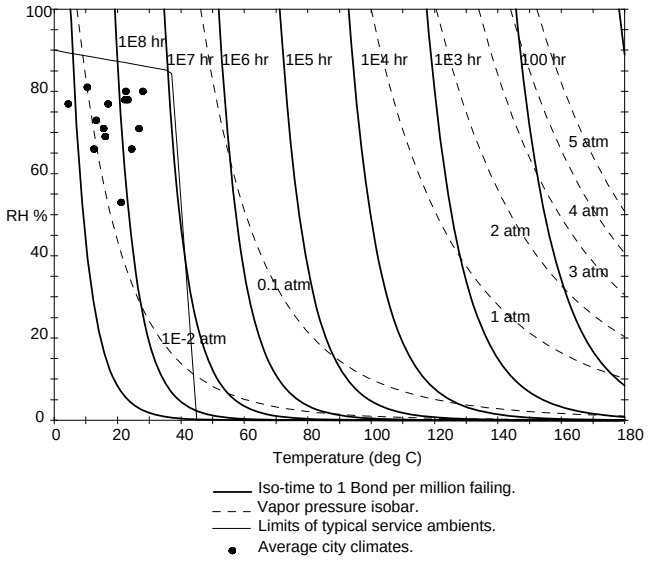

Fig. 10 Model predictions for time to 1 bond per million with shear strength < 25 grams. Worst-case model parameters were assumed (polyimide, 25% off-pad). Also shown is the range of typical service ambients, and climates of various world cities. Water vapor pressure isobars are also superimposed.

Acknowledgments

The authors would like to express their deep gratitude to Jeanie Vierra and Tim Boyer for the incredible amount of time and work they put into running the factorial experiments. Thanks are also expressed to Bertha Jones, Julio Tribiana and Deepak Goyal for their analytic services, and to Gay Samuelson for her technical support.

References

[1] T. Hund, "Thermosonic Gold-Ball Bond Accelerated Life Test," in Proc. 40th Electronic Components & Technology Conference, May 1990, pp436-441.

[2] A. Gallo, "Effect of Mold Compound Components on Moisture-Induced Degradation of Gold-Aluminum Bonds in Epoxy Encapsulated Devices," in 28th Annual Proc., Reliability Physics, March 1990, pp. 244-251.

[3] E. Philofsky, "Intermetallic Formation in Gold-Aluminum Systems," Solid State Electronics, Vol. 13, pp1391-1399, 1970.

[4] W. Gerling, "Electrical and Physical Characterization of Gold-Ball Bonds on Aluminum Layers," in IEEE Electronic Components Conference, 1984, pp13-20.

[5] T. Ramsey, C. Alfaro, and H. Dowell, "Metallurgy's Part in Gold Ball Bonding," Semiconductor International, pp98-102, April 1991.

[6] R. C. Blish and L. Parobeck, "Wire Bond Integrity Test Chip," in Proc. 21st Annual Proceedings International Reliability Physics Symposium, 1983, pp. 142-147.

[7] M. Shell-De Guzman and M. Mahaney, "The Bond Shear Test: An Application for the Reduction of Common Causes of Gold Ball Bond Process Variation," in 30th Annual Proc., Reliability Physics, March 1992, pp. 251-257.

[8] The more severe bond degradation seen after 40 hours in 156/85 HAST as compared with that shown in Table III below is due to the fact that the material was assembled at a different time with different bonding parameters. We will see in Section 5 that degradation in stress is very sensitive to bonder force settings.

[9] S. Groothuis, W. Schroen and M. Murtuza, "Computer Aided Stress Modeling for Optimizing Plastic Package Reliability," in Proc. 23rd Annual Proceedings International Reliability Physics Symposium, 1985, pp. 184-191.

[10] W. Nelson, Applied Life Data Analysis. New York: Wiley, 1982, pp173-192.

[11] D. S. Peck, "Comprehensive Model for Humidity Testing Correlation," in Proc. 24th Ann. Int'l Reliability Physics Symposium, 1986, pp44-50

[12] A two-dimensional least-squares regression fit of $\log_{10}a$ versus $\log_{10}h$ and $1/T$ was done using the transformation of Eq. (3):

$$\log_{10} a = \log_{10} a_0 + p \times \log_{10} h - 0.43429 \times Q \times k^{-1} \times (1/T)$$

$\log_{10}a_0$, p and Q are the coefficients which minimize the sum of squares of deviation of the model from the data.